

Performance Analysis of Prerake DS UWB Multiple Access System Under Imperfect Channel Estimation

Wei Cao, *Student Member, IEEE*, A. Nallanathan, *Senior Member, IEEE*,
and Chin Choy Chai, *Member, IEEE*

Abstract—In this paper, the performance of Prerake DS UWB multiple access system under imperfect channel estimation is studied. The signal model of the system is derived in matrix form, which clearly shows the components of inter-chip interference, inter-symbol interference and multiple access interference. The BER formula is derived based on this signal model and validated by simulations. We highlight that the BER performance does not monotonically decrease with the growth of data rate under imperfect channel estimation. The effect of imperfect channel estimation in different cases is also discussed.

Index Terms—Prerake, DS UWB, imperfect channel estimation, multiple access, signal model, BER.

I. INTRODUCTION

DUE to the dense multipath channels, effective energy capture is a challenging task in UWB communications. In order to effectively capture the energy with a simple receiver structure, the Prerake technique (also named Time Reversal) has been investigated for UWB communications. In [1], simulation results show that the Pre-Rake and Rake combining achieve almost the same BER performance when the number of taps in the Pre-Rake filter equals to the number of fingers in the Rake receiver. A Time-Reversal MMSE equalizer for UWB communications is proposed in [2] to optimally combine the energy in several taps. In [3], the zero-forcing optimization for a prerake UWB system in the presence of inter-pulse interference and narrow-band interference is studied. In all these works mentioned above, single user scenario and perfect channel estimation are the basic assumptions. In [4], a low-complexity Time Reversal prefilter is proposed using a 3-level A/D conversion to simplify the channel estimation, and system performance is examined in a single user scenario. Since multiple access interference (MAI) is one of the major difference between Prerake and Rake systems [5], it is of interest to study the Prerake UWB multiple access systems. Currently, little work has been done on the Prerake UWB system with multiple users under imperfect channel estimation. In this paper, the analytical signal model for a Prerake DS UWB multiple access system under imperfect channel estimation is presented for the first time. The BER formula is derived based on this model. The effect of imperfect

channel estimation on the system performance is discussed in detail.

II. SYSTEM MODEL

A. Channel Model

According to [6], the channel impulse response of the k^{th} user is modeled as

$$h^{(k)}(t) = \sum_{l=0}^{L-1} \alpha_{l,k} \delta(t - \tau_{l,k}) \quad (1)$$

where L is the number of paths in the channel. The path gain $\alpha_{l,k} = \theta_{l,k} \beta_{l,k}$, where $\theta_{l,k}$ is equiprobable ± 1 to account for pulse inversion due to reflection and $\beta_{l,k}$ is the lognormal fading amplitude. For different k and l , $\alpha_{l,k}$ are independent random variables. We consider the resolvable multipath channel with $\tau_{l,k} = \tau_{0,k} + lT_p$, where T_p is the width of UWB monocycle $z(t)$. Since multipath components tend to arrive in clusters [6], the l^{th} path can be expressed as the j^{th} ray in the i^{th} cluster. Therefore, delay of the l^{th} path $\tau_{l,k} = \mu_{i,k} + \nu_{j,i,k}$, where $\mu_{i,k}$ is delay of the i^{th} cluster and $\nu_{j,i,k}$ is delay of the j^{th} ray in the i^{th} cluster relative to $\mu_{i,k}$. The power delay profile of the channel is double exponential decaying by rays and clusters. Since the transmitter and receiver are stationary in most personal area networks (PAN) applications [6], the channel is assumed to remain constant over a block of symbols.

B. Transmitted Signal

The transmitted signal due to the k^{th} user is

$$\tilde{s}^{(k)}(t) = A_k \sum_{i=-\infty}^{\infty} b_i^k x^{(k)}(t - iT_r) \quad (2)$$

where T_r is the symbol duration, A_k denotes the amplitude, $b_i^k \in \{\pm 1\}$ is the i^{th} symbol. In the DS UWB multiple access system, the symbol waveform of the k^{th} user is given by

$$x^{(k)}(t) = \sum_{n=0}^{N_r-1} a_n^k g^{(k)}(t - nT_c) \quad (3)$$

where $\{a_n^k\}_{n=0}^{N_r-1}$ is the DS signature assigned to the k^{th} user and $T_c = T_r/N_r$ is the chip duration. The chip waveform $g^{(k)}(t)$ is formed by passing $z(t)$ through a Prerake filter $\tilde{h}^{(k)}(t)$.

$$g^{(k)}(t) = z(t) * \tilde{h}^{(k)}(t) = \sum_{l=0}^{L_c-1} \tilde{\alpha}_{L_c-1-l,k} z(t - lT_p) \quad (4)$$

where $z(t)$ is the UWB monocycle of duration T_p with normalized energy. The Prerake filter $\tilde{h}^{(k)}(t) =$

Manuscript received May 28, 2006; revised November 9, 2006 and January 15, 2007; accepted February 19, 2007. The editor coordinating the review of this paper and approving it for publications is Prof. E. Serpedin.

W. Cao and A. Nallanathan are with the Department of Electrical and Computer Engineering, National University of Singapore, Singapore (email: {caowei, elena}@nus.edu.sg).

C. C. Chai is with the Institute for Infocomm Research, Singapore (email: chaicc@i2r.a-star.edu.sg).

Digital Object Identifier 10.1109/TWC.2007.060301.

$\sum_{l=0}^{L_c-1} \tilde{\alpha}_{L_c-1-l,k} \delta(t - lT_p)$ contains L_c taps and the chip duration $T_c = L_c T_p$. Following the concept of All-Prerake and Partial-Prerake schemes introduced in [7], a data rate increasing factor N_c is defined as a submultiple of L , i.e., $L = N_c L_c$. In the All-Prerake scheme, $N_c = 1$ and data rate is $R_b = 1/(N_r L T_p)$. In the Partial-Prerake scheme, $N_c > 1$ and the data rate is $R_b = N_c/(N_r L T_p)$, which is N_c times of the data rate in All-Prerake scheme. In $\tilde{h}^{(k)}(t)$, $\{\tilde{\alpha}_{l,k}\}_{l=0}^{L_c-1}$ is the estimated value of channel gain $\{\alpha_{l,k}\}_{l=0}^{L_c-1}$.

The amplitude $A_k = \sqrt{E_p / \sum_{l=0}^{L_c-1} \mathbb{E} [\tilde{\alpha}_{l,k}^2]}$ is to keep the average transmitted symbol energy constant as $E_b = N_r E_p$.

C. Received Signal

The received signal due to the k^{th} user is given by

$$\begin{aligned}
 r^{(k)}(t) &= \tilde{s}^{(k)}(t) * h^{(k)}(t) \\
 &= A_k \sum_{i=-\infty}^{\infty} b_i^k \underbrace{\left[x^{(k)}(t - iT_r) * h^{(k)}(t) \right]}_{\tilde{x}^{(k)}(t - iT_r)} \quad (5)
 \end{aligned}$$

where $\tilde{x}^{(k)}(t)$ is obtained using (3) as

$$\begin{aligned}
 \tilde{x}^{(k)}(t) &\triangleq x^{(k)}(t) * h^{(k)}(t) \\
 &= \sum_{n=0}^{N_r-1} a_n^k \underbrace{\left[g^{(k)}(t - nT_c) * h^{(k)}(t) \right]}_{\tilde{g}^{(k)}(t - nT_c)} \quad (6)
 \end{aligned}$$

where $\tilde{g}^{(k)}(t) \triangleq g^{(k)}(t) * h^{(k)}(t)$ is the channel response of a chip waveform $g^{(k)}(t)$.

The total received signal in a K -user system with asynchronous transmission is given by

$$r(t) = \sum_{k=0}^{K-1} r^{(k)}(t - \tau_{0,k}) + n(t) \quad (7)$$

where $n(t)$ is AWGN with two-sided power spectrum density of $N_0/2$ and $\tau_{0,k}$ serves as the transmission delay of the k^{th} user. Since random DS sequences/data bits are assumed, the interfering users appear to the desired user as essentially transmitting random $\{\pm 1\}$ sequences and the boundaries of interfering symbols do not matter in asynchronous transmission. This property allows us to assume that $\tau_{0,k}$ is uniformly distributed in $[0, T_c)$.

D. Channel Estimation

The estimated channel gains $\{\tilde{\alpha}_{l,k}\}_{l=0}^{L_c-1}$ are obtained by a time domain channel estimation scheme. We assume all other users keep silent during channel estimation period of the k^{th} user. The k^{th} user sends N_t training UWB monocycles $z(t)$. The training monocycle repetition interval is larger than the maximum delay spread of the channel to avoid interference between training monocycles. Assuming perfect synchronization, the base station correlates and samples at the tap rate on the i^{th} received training monocycle to get the estimated channel gain on the first L_c paths.

$$\tilde{\alpha}_{l,k}(i) = \int_{lT_p}^{(l+1)T_p} \left(\sum_{l'=0}^{L_c-1} \alpha_{l',k} z(t - l'T_p) + n_i(t) \right) z(t - lT_p) dt$$

where $i = 0, 1, \dots, N_t - 1$ is the index of training monocycles. Then N_t estimation results are averaged to obtain the

estimated channel gain as follows.

$$\tilde{\alpha}_{l,k} = \frac{1}{N_t} \sum_{i=0}^{N_t-1} \tilde{\alpha}_{l,k}(i) = \alpha_{l,k} + n_{l,k} \quad (8)$$

where $n_{l,k} \sim \text{Gaussian}(0, \frac{N_0}{2N_t})$ is the noise brought by imperfect channel estimation on the l^{th} path. Since total L_c paths are to be estimated, larger L_c will lead to stronger impact of imperfect channel estimation.

III. SIGNAL MODELING AND DECISION STATISTICS

A. Signal Modeling

The channel gain and the estimated channel gain used in the Prerake filter are defined as vectors

$$\begin{aligned}
 \alpha_k &= (\alpha_{0,k} \quad \alpha_{1,k} \quad \dots \quad \alpha_{L-1,k})^T \\
 \tilde{\alpha}_k &= (\tilde{\alpha}_{L_c-1,k} \quad \tilde{\alpha}_{L_c-2,k} \quad \dots \quad \tilde{\alpha}_{0,k})^T
 \end{aligned}$$

$\tilde{g}^{(k)}(t)$ in (6) can be discretized by $\tilde{g}_{j,k} = \int_{jT_p}^{(j+1)T_p} \tilde{g}^{(k)}(t) z(t - jT_p) dt$ and expressed as

$$\tilde{\mathbf{g}}_k = \mathbf{T}_{\alpha_k} \tilde{\alpha}_k = (\tilde{g}_{0,k} \quad \tilde{g}_{1,k} \quad \dots \quad \tilde{g}_{L+L_c-2,k})^T \quad (9)$$

where \mathbf{T}_{α_k} is a $(L + L_c - 1) \times L_c$ Toeplitz matrix with α_k as the first L elements in its 0^{th} column and zero elsewhere. Note that $\tilde{\mathbf{g}}_k$ includes the effect of imperfect channel estimation and

the element $\tilde{g}_{L_c-1,k} = \sum_{l=0}^{L_c-1} \alpha_{l,k} \tilde{\alpha}_{l,k}$ is the desired peak.

Another Toeplitz matrix $\mathbf{T}_{\mathbf{a}_k}$ of size $(2N_r L_c) \times (L + L_c - 1)$ is defined using the DS code $\{a_n^k\}_{n=0}^{N_r-1}$. The 0^{th} column of $\mathbf{T}_{\mathbf{a}_k}$ contains $(a_0^k \quad \mathbf{0}_{L_c-1} \quad a_1^k \quad \mathbf{0}_{L_c-1} \quad \dots \quad a_{N_r-1}^k \quad \mathbf{0}_{L_c-1})^T$ as the first $N_r L_c$ elements and zero elsewhere, where $\mathbf{0}_{L_c-1}$ denotes the zero vector with $L_c - 1$ elements. Next, $\mathbf{T}_{\mathbf{a}_k}$ is split into two $(N_r L_c) \times (L + L_c - 1)$ matrices: $\mathbf{T}_{\mathbf{a}_{k,0}}$ consists of the upper half of $\mathbf{T}_{\mathbf{a}_k}$ from the 0^{th} row to the $(N_r L_c - 1)^{th}$ row, and $\mathbf{T}_{\mathbf{a}_{k,1}}$ consists of the lower half of $\mathbf{T}_{\mathbf{a}_k}$ from the $(N_r L_c)^{th}$ row to the $(2N_r L_c - 1)^{th}$ row.

In order to convert the continuous-time signal $r^{(k)}(t)$ into a discrete format, $r^{(k)}(t)$ is filtered by a tap-matched filter $z(t)$ and then sampled at the tap rate. Therefore each symbol consists of $N_r L_c$ samples. Without loss of generality, we assume that the 0^{th} symbol is the desired symbol. The received discrete symbol can be expressed as

$$\begin{aligned}
 \mathbf{r}_k &= (r_0^k \quad r_1^k \quad \dots \quad r_{N_r L_c-1}^k)^T \\
 &= A_k \mathbf{T}_{\mathbf{a}_{k,0}} \tilde{\mathbf{g}}_k b_0^k + A_k \mathbf{T}_{\mathbf{a}_{k,1}} \tilde{\mathbf{g}}_k b_{-1}^k \quad (10)
 \end{aligned}$$

B. Decision Statistics

We assume that the 0^{th} user is the desired user. To detect the 0^{th} symbol, the 0^{th} receiver performs correlation on the N_r peaks in the received signal $r(t)$. The output is given by

$$\begin{aligned}
 Z &= \underbrace{\int_0^{T_r} r^{(0)}(t) v^{(0)}(t) dt}_{S+I_C+I_S} + \underbrace{\int_0^{T_r} n(t) v^{(0)}(t) dt}_N \\
 &+ \underbrace{\sum_{k=1}^{K-1} \int_0^{T_r} r^{(k)}(t - \tau_{0,k}) v^{(0)}(t) dt}_{I_M} \quad (11)
 \end{aligned}$$

where $v^{(0)}(t) = \sum_{n=0}^{N_r-1} a_n^0 z(t - nT_c - (L_c - 1)T_p)$ is the template waveform in the 0th receiver. The output Z can be decomposed as desired signal S , inter-chip interference I_C , inter-symbol interference I_S , multiple access interference I_M and AWGN term N .

B.1. Desired Signal, Inter-Chip Interference and Inter-Symbol Interference

Similar to $r^{(k)}(t)$, the template waveform $v^{(0)}(t)$ can be expressed in discrete format as $\mathbf{v}_0 = (\mathbf{0}_{L_c-1} \ a_0^0 \ \mathbf{0}_{L_c-1} \ a_1^0 \ \cdots \ \mathbf{0}_{L_c-1} \ a_{N_r-1}^0)$. The first term in (11) can be rewritten as

$$S + I_C + I_S = \mathbf{v}_0 \mathbf{r}_0 = \underbrace{A_0 \mathbf{v}_0 \mathbf{T}_{\mathbf{a}_{0,0}} \tilde{\mathbf{g}}_0 b_0^0}_{S + I_C} + \underbrace{A_0 \mathbf{v}_0 \mathbf{T}_{\mathbf{a}_{0,1}} \tilde{\mathbf{g}}_0 b_{-1}^0}_{I_S} \quad (12)$$

Recall the fact that $\tilde{g}_{L_c-1,0}$ is the peak containing the desired signal energy. S and I_C can be expressed as below, where both terms contain imperfect channel estimation effect brought by $\tilde{\mathbf{g}}_0$.

$$\begin{aligned} S &= A_0 \mathbf{v}_0 \mathbf{T}_{\mathbf{a}_{0,0}} \tilde{\mathbf{g}}_0 b_0^0 \\ I_C &= A_0 \mathbf{v}_0 \mathbf{T}_{\mathbf{a}_{0,0}} (\tilde{\mathbf{g}}_0 - \tilde{\mathbf{g}}_0') b_0^0 \end{aligned} \quad (13)$$

where $\tilde{\mathbf{g}}_0'$ is obtained by setting all elements in $\tilde{\mathbf{g}}_0$ as zeros except the element $\tilde{g}_{L_c-1,0}$.

B.2. Multiple Access Interference

In pervious work on Prerake TDD/CDMA [8], the imperfect channel estimation in MAI is ignored to avoid computational complexity. However, the imperfect channel estimation leads to interference energy distraction and changes the statistical property of MAI. Therefore we consider the imperfect channel estimation effect in I_M . From (11), $I_M = \sum_{k=1}^{K-1} I_{M,k}$, where $I_{M,k}$ is the interference from the k^{th} interfering user. $I_{M,k}$ comes from either one or two adjacent symbols. We add the index i in (10) to indicate the i^{th} symbol of the k^{th} user.

$$\begin{aligned} \mathbf{r}_k(i) &= (r_0^k(i) \ r_1^k(i) \ \cdots \ r_{N_r L_c - 1}^k(i))^T \\ &= A_k \mathbf{T}_{\mathbf{a}_{k,0}} \tilde{\mathbf{g}}_k b_i^k + A_k \mathbf{T}_{\mathbf{a}_{k,1}} \tilde{\mathbf{g}}_k b_{i-1}^k \end{aligned} \quad (14)$$

The asynchronous delay $\tau_{0,k}$ can be split as $\tau_{0,k} = \gamma_k T_p + \Delta T_k$, where $\gamma_k \in \{0, 1, \dots, L_c - 1\}$ and $\Delta T_k \in [0, T_p)$, both with uniform distribution. The partial correlation functions of $z(t)$ is defined as $P(x) = \int_0^x z(t) z(t + T_p - x) dt$. Then $I_{M,k}$ is given by

$$I_{M,k} = \mathbf{v}_0 \mathbf{R}_{k,0} P(\Delta T_k) + \mathbf{v}_0 \mathbf{R}_{k,1} P(T_p - \Delta T_k) \quad (15)$$

where

$$\mathbf{R}_{k,x} = (r_{N_r L_c - \gamma_k - 1 + x}^k(-1) \ \cdots \ r_{N_r L_c - 1}^k(-1) \ r_0^k(0) \ \cdots \ r_{N_r L_c - \gamma_k - 2 + x}^k(0))^T \quad (16)$$

IV. BER PERFORMANCE ANALYSIS

Since the path number L is large, we use the Gaussian approximation in following analysis. Set total noise $\varsigma = I_C + I_S + I_M + N$. It is easy to check that all terms in ς have zero mean and are independent conditioned on α_0 and $\tilde{\alpha}_0$. The instantaneous SINR is defined as

$$\gamma = \frac{S^2}{\sigma_\varsigma^2} = \frac{S^2}{\sigma_{I_C}^2 + \sigma_{I_S}^2 + \sigma_{I_M}^2 + N_0 N_r / 2} \quad (17)$$

where

$$S^2 = A_0^2 \mathbf{v}_0 \mathbf{T}_{\mathbf{a}_{0,0}} \tilde{\mathbf{g}}_0 \tilde{\mathbf{g}}_0' T \mathbf{T}_{\mathbf{a}_{0,0}}^T \mathbf{v}_0^T = A_0^2 N_r^2 \tilde{g}_{L_c-1,0}^2 \quad (18)$$

$$\begin{aligned} \sigma_{I_C}^2 + \sigma_{I_S}^2 &= A_0^2 \mathbb{E} \left[\mathbf{v}_0 \mathbf{T}_{\mathbf{a}_{0,0}} (\tilde{\mathbf{g}}_0 - \tilde{\mathbf{g}}_0') (\tilde{\mathbf{g}}_0 - \tilde{\mathbf{g}}_0')^T \mathbf{T}_{\mathbf{a}_{0,0}}^T \mathbf{v}_0^T \right] \\ &\quad + A_0^2 \mathbb{E} \left[\mathbf{v}_0 \mathbf{T}_{\mathbf{a}_{0,1}} \tilde{\mathbf{g}}_0 \tilde{\mathbf{g}}_0^T \mathbf{T}_{\mathbf{a}_{0,1}}^T \mathbf{v}_0^T \right] \\ &= A_0^2 N_r \sum_{j=2}^{N_c} \tilde{g}_{j L_c - 1,0}^2 \end{aligned} \quad (19)$$

In calculation of $\sigma_{I_M}^2$, we use $\mathbb{E}[P(\Delta T_k) P(T_p - \Delta T_k)] \approx 0$ to simplify the expression.

$$\begin{aligned} \sigma_{I_M}^2 &= (K-1) \sigma_{I_{M,k}}^2 = \frac{2(K-1)}{L_c} \mathbb{E} [P^2(\Delta T_k)] \mathbb{E} [\mathbf{r}_k^T \mathbf{r}_k] \\ &= \frac{2(K-1)}{L_c} \mathbb{E} [P^2(\Delta T_k)] A_k^2 N_r \sum_{j=0}^{L+L_c-2} \mathbb{E} [\tilde{g}_{j,k}^2] \end{aligned} \quad (20)$$

where

$$\begin{aligned} \mathbb{E} [\tilde{g}_{j,k}^2]_{j \neq L_c-1} &= \sum_{n=\max[0, j-L+1]}^{\min[j, L_c-1]} \mathbb{E} [\alpha_{j-n,k}^2] \mathbb{E} [\alpha_{L_c-1-n,k}^2] \\ &\quad + \frac{N_0}{2N_t} \sum_{n=\max[0, j-L+1]}^{\min[j, L_c-1]} \mathbb{E} [\alpha_{j-n,k}^2] \\ \mathbb{E} [\tilde{g}_{L_c-1,k}^2] &= \sum_{n=0}^{L_c-1} \mathbb{E} [\alpha_{n,k}^4] + \sum_{n=0}^{L_c-1} \sum_{\substack{n'=0 \\ n' \neq n}}^{L_c-1} \mathbb{E} [\alpha_{n,k}^2] \mathbb{E} [\alpha_{n',k}^2] \\ &\quad + \frac{N_0}{2N_t} \sum_{n=0}^{L_c-1} \mathbb{E} [\alpha_{n,k}^2] \end{aligned}$$

The x^{th} moment of $\alpha_{l,k}$ can be obtained by the x^{th} moment of $\beta_{l,k}$, i.e., $\mathbb{E}[(\beta_{l,k})^x] = \exp(x \eta_{y_{l,k}} + x^2 \sigma_{y_{l,k}}^2 / 2)$, where $\beta_{l,k} = \exp(y_{l,k})$ and $y_{l,k} \sim \text{Gaussian}(\eta_{y_{l,k}}, \sigma_{y_{l,k}}^2)$.

The average BER P_{Average} is obtained by averaging the instantaneous BER $P_{\text{Instant}}(\gamma)$ over the distribution of the instantaneous SINR γ .

$$P_{\text{Instant}}(\gamma) = \frac{1}{2} \text{erfc} \left(\sqrt{\frac{\gamma}{2}} \right) \quad (21)$$

$$P_{\text{Average}} = \int_0^\infty P_{\text{Instant}}(\gamma) p_\gamma(\gamma) d\gamma$$

where $p_\gamma(\gamma)$ is the probability density function of the instantaneous SINR at the output of the correlator receiver. In Section V, we compute the average BER using the Monte Carlo method.

V. NUMERICAL RESULTS AND DISCUSSION

In Table I, the channel parameters are listed according to [6]. The UWB monocycle is $z(t) = \varepsilon \left[1 - 4\pi \left(\frac{t - T_p/2}{\tau_p} \right)^2 \right] \exp \left[-2\pi \left(\frac{t - T_p/2}{\tau_p} \right)^2 \right]$, where $T_p = 0.25\text{ns}$, $\tau_p = 0.10275\text{ns}$ and $\varepsilon = 1.6111 \times 10^5$. The length of the DS sequence is $N_r = 16$. Different values of the data rate increasing factor $N_c = 1, 4, 8, 20$ are used. With the growth of N_c , the bit rate R_b increases. For the

TABLE I
THE PARAMETERS USED IN NUMERICAL STUDY

Model Parameters	CM1	CM3
Γ_1 (cluster power decay factor)	7.1	14
Γ_2 (ray power decay factor)	4.3	7.9
σ_1 (stand. dev. of cluster lognormal fading in dB)	3.3941	3.3941
σ_2 (stand. dev. of ray lognormal fading in dB)	3.3941	3.3941
L (path number)	200	400
R_b (Mbps) when $N_c = 1$	1.25	0.625
R_b (Mbps) when $N_c = 4$	5	2.5
R_b (Mbps) when $N_c = 8$	10	5
R_b (Mbps) when $N_c = 20$	25	12.5

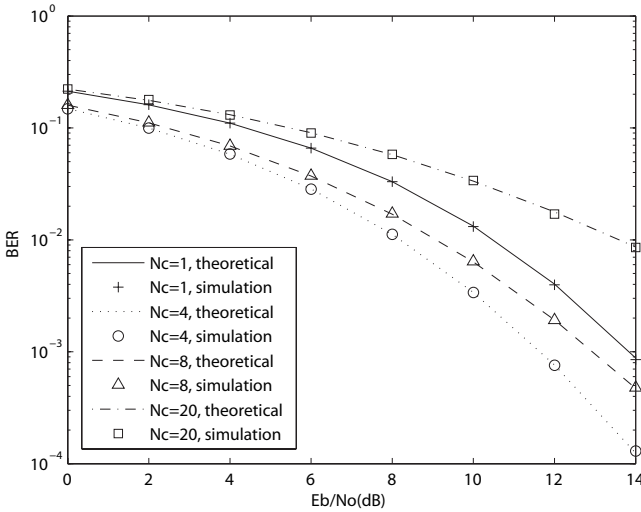


Fig. 1. BER performance of the Prerake DS UWB system in UWB channel model CM1 under imperfect channel estimation, the data rate increasing factor $N_c = 1, 4, 8, 20$, the number of users $K = 1$, the number of training monocycles $N_t = 100$.

same N_c value, R_b in CM1 is larger than in CM3 because of the smaller maximal delay spread of CM1.

In Fig. 1, the theoretical and simulation BER results are shown for a single user scenario in CM1. It is found that the BER value is a concave function of N_c because of the imperfect channel estimation effect. When N_c is small (e.g. $N_c = 1, 4$), AWGN dominates the total noise and SINR can be approximated as $\gamma \approx 2A_0^2 N_r \tilde{g}_{L_c-1,0}^2 / N_0$. The growth of N_c makes A_0^2 grows faster than the decrease of $\tilde{g}_{L_c-1,0}^2$, which results in larger γ and better BER performance. However, the sum of ICI and ISI becomes dominant when N_c is large (e.g. $N_c = 8, 20$). Then SINR can be approximated as $\gamma \approx N_r \tilde{g}_{L_c-1,0}^2 / \sum_{j=2}^{N_c} \tilde{g}_{jL_c-1,0}^2$, and the growth of N_c leads to less desired signal energy and larger ICI and ISI. Therefore BER performance degrades with the growth of N_c .

In Fig. 2, the BER performance in multiple user scenario is shown in CM1. In low SNR (E_b/N_0) range, the BER performance of $N_c = 1$ is worse than $N_c = 8$ for both $K = 10, 50$. With the increase of SNR, the BER performance of $N_c = 1$ gets better than $N_c = 8$. This reflects the impact of imperfect channel estimation under different SNR. In low SNR range, AWGN dominates the total noise so that the growth of N_c brings better BER performance by decreasing

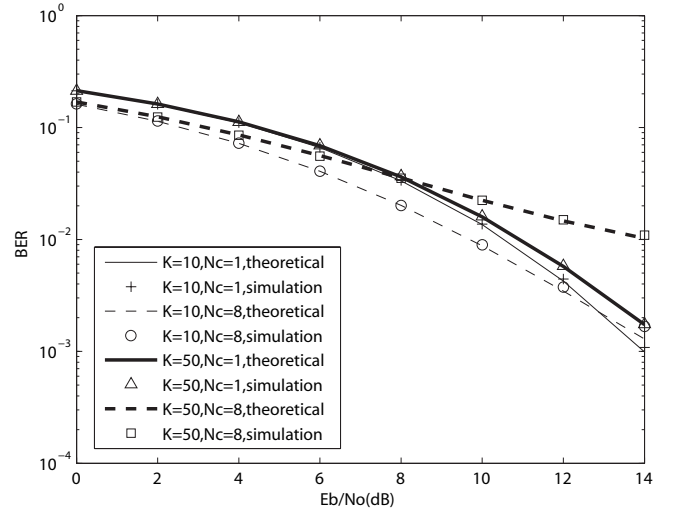


Fig. 2. BER performance of the Prerake DS UWB system in UWB channel model CM1 under imperfect channel estimation, the data rate increasing factor $N_c = 1, 8$, the number of users $K = 10, 50$, the number of training monocycles $N_t = 100$.

the effect of imperfect channel estimation. On the other hand, the dominating factor in the total noise becomes the sum of ICI, ISI and MAI in high SNR range, so the BER performance of $N_c = 8$ is worse than $N_c = 1$ because of stronger interference brought by larger N_c value. The BER curves of $N_c = 1$ and $N_c = 8$ intersect at about $E_b/N_0 = 8$ dB and 12 dB for $K = 10$ and 50 respectively. This shows that the growth of SNR brings larger MAI increment when the number of users is larger.

In Fig. 3, the BER curves for $K = 50$ in CM1 are plotted under perfect and imperfect channel estimation. As expected, larger N_t brings better BER performance because that the variance of $n_{l,k}$ in (8) gets smaller as N_t increases. For a desired BER of 10^{-3} , the SNR gain between $N_t = 200$ and $N_t = \infty$ is around 3.5 dB. Another finding is that when N_c is larger, the BER gap between imperfect and perfect channel estimation becomes smaller. The reason is that larger N_c corresponds to smaller L_c and the impact of imperfect channel estimation is in proportion to L_c .

In Fig. 4, the BER performance is depicted as a function of the number of multiple access users under perfect and imperfect channel estimation. The SNR value is fixed as 14 dB. With the increase of number of users, the BER value increases as expected. The BER performance in CM3 is better than in CM1 under perfect channel estimation, which is consistent with the results in [9]. When the number of training monocycles in channel estimation $N_t = 100$, the BER performance in CM1 is better than in CM3. This indicates that imperfect channel estimation exerts more unfavorable influence on the BER performance in CM3 due to the larger number of paths.

In time domain channel estimation, larger number or higher power of the training monocycles would lead to more accurate channel estimation and improve the system performance. Besides the time domain channel estimation, the combined frequency domain channel estimation/equalization [10] could be a promising candidate to achieve better system performance.

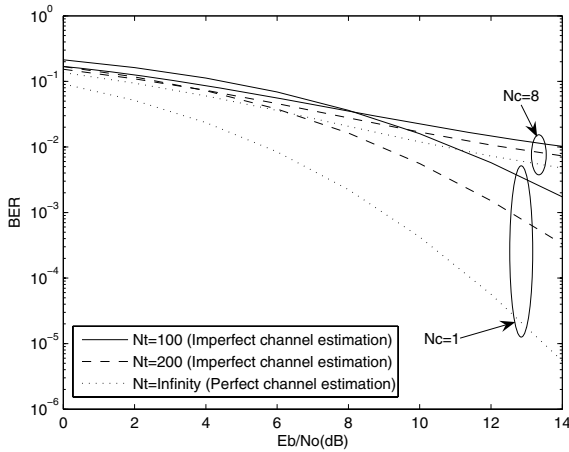


Fig. 3. BER performance of the Prerake DS UWB system in UWB channel model CM1 under imperfect and perfect channel estimation, the data rate increasing factor $N_c = 1, 8$, the number of users $K = 50$, the number of training monocycles $N_t = 100, 200, \infty$.

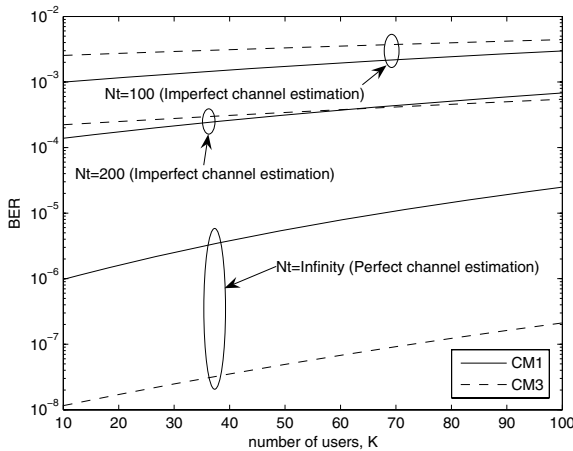


Fig. 4. BER performance of the Prerake DS UWB system in UWB channel model CM1 and CM3 with different number of users, the data rate increasing factor $N_c = 1$, the number of training monocycles $N_t = 100, 200, \infty$.

VI. CONCLUSIONS

We study the performance of Prerake DS UWB multiple access systems under imperfect channel estimation. The

analytical signal model of the system is derived, which clearly presents the components of inter-chip interference, inter-symbol interference and multiple access interference. The derivation of statistical property of interference provides theoretical basis for the future work on interference suppression. The BER formula is derived based on the signal model and verified by numerical results. Under perfect channel estimation, the BER performance degrades with the growth of data rate. However, the BER performance does not decrease monotonically with the increase of data rate under imperfect channel estimation. The BER performance depends on the dominating factor in SINR, which is a combined result of SNR, channel estimation and number of users. Generally, the imperfect channel estimation exerts more unfavorable influence on the BER performance when the data rate is lower or in a channel with larger number of multipaths.

REFERENCES

- [1] K. Usuda, H. Zhang, and M. Nakagawa, "Pre-RAKE diversity combining for UWB systems in IEEE 802.15 UWB multipath channel," in *Proc. IEEE WCNC*, May 2004, pp. 236–240.
- [2] T. Strohmer, M. Emami, J. Hansen, G. Papanicolaou, and A. J. Paulraj, "Application of time-reversal with MMSE equalizer to UWB communications," in *Proc. IEEE GLOBECOM*, Nov. 2004, pp. 3123–3127.
- [3] S. Zhao and H. Liu, "Pre-RAKE diversity combining for pulsed UWB systems considering realistic channels with pulse overlapping and narrow-band interference," in *Proc. IEEE GLOBECOM*, Nov. 2005, pp. 3784–3788.
- [4] N. Guo, R. C. Qiu, and B. M. Sadler, "An ultra-wideband autocorrelation demodulation scheme with low-complexity time reversal enhancement," in *Proc. MILCOM 2005*, Oct. 2005, pp. 1–7.
- [5] R. Esmailzadeh, E. Sourour, and M. Nakagawa, "PreRAKE diversity combining in time-division duplex CDMA mobile communications," *IEEE Trans. Veh. Technol.*, vol. 48, no. 3, pp. 795–801, May 1999.
- [6] J. R. Foerster, "Channel modeling sub-committee report final (doc: IEEE 802-15-02/490r1-sg3a)," Feb. 2002.
- [7] S. Imada and T. Ohtsuki, "Pre-RAKE diversity combining for UWB systems in IEEE 802.15 UWB multipath channel," in *Proc. Joint UWBST and IWUWBS*, May 2004, pp. 236–240.
- [8] S. E. El-Khamy, E. E. Sourour, and T. A. Kadous, "Wireless portable communications using pre-RAKE CDMA/TDD/QPSK systems with different combining techniques and imperfect channel estimation," in *Proc. IEEE PIMRC 1997*, Sept. 1997, pp. 529–533.
- [9] W. Cao, A. Nallanathan, and C. C. Chai, "On the multiple access performance of Prerake DS UWB System," in *Proc. Milcom*, Oct 2006.
- [10] Y. Wang and X. Dong, "Frequency domain channel estimation for SC-FDE in UWB communications," *IEEE Trans. Commun.*, vol. 54, no. 12, pp. 2155–2163, Dec. 2006.